

Signal analysis of the post-Newtonian gravitational wave form of coalescing binaries

Kanti Jotania,* Sanjay M. Wagh, and Sanjeev V. Dhurandhar†

Inter-University Centre for Astronomy and Astrophysics, Post Bag 4, Ganeshkhind, Pune 411 007, India

(Received 28 February 1992)

In this paper we compute the signal-to-noise ratios for gravitational wave signals from coalescing binaries in the post-Newtonian approximation using matched-filtering techniques. We find that, up to the second post-Newtonian order, on the whole the signal-to-noise ratios are reduced for broadband detectors. For a binary with a mass parameter $\sim 1M_{\odot}$ and detection frequency range of 100–2000 Hz the signal-to-noise ratio can go down by as much as 15%. This is basically due to the reduction in integration time of the signal. We compute the signal-to-noise ratios in the standard recycling case for a wide range of parameters which include the orientation of the detector and source. Useful semianalytic formulas are derived. Numerical results are displayed for the full wave form for various orientations of the binary system.

PACS number(s): 04.30.+x, 04.80.+z, 06.50.Dc, 97.80.Fk

I. INTRODUCTION

The question of gravitational radiation (GR) emitted by matter has always been one of the central problems of the general theory of relativity (GTR). With the latest technological advances which have brought the detection of GR within the realm of modern scientific instrumentation, this central problem of the GTR has certainly become one of the most important problems of present-day science. The firm detection of GR will allow us to not only conduct far-reaching tests of the GTR in the strong-field regime of the theory but also to explore the history in time of the Universe to unprecedented epochs in the past. Such problems of astronomy as the theory of galaxy formation and the formation and existence of black holes, to name two, would be amenable to definitive tests which could then be expected to select one of the many alternative scenarios.

This radiation, which is basically a transverse, quadrupole wave (a ripple on spacetime) propagating at the speed of light, is generated when a time-dependent mass quadrupole is produced by the motion of matter. The gravitational waves thus produced, if incident on a laser interferometric gravitational wave detector, effectively change the arm lengths of an interferometer. The dimensionless amplitude h of GR is then related to the response of the laser interferometer as $h \sim \delta l / l$, where l is the proper distance between prearranged test masses of the detector and δl is the change in that distance caused by GR incident on that detector. A typical value of h expected from a strong astrophysical source such as a supernova is $\sim 10^{-18}$ – 10^{-21} , indicating that a change of order $\lesssim 10^{-13}$ cm would be produced in a detector that has test masses about 1 km apart. Needless to say, the

most important sources of GR would be then those in which the quadrupole moment of matter changes rapidly and, therefore, produces radiation (of sufficient intensity and amplitude) which could be detected using such detectors. It is then imperative for us to explore the possible strong sources of GR.

As an example, a supernova explosion could be a strong emitter of GR if the collapse and subsequent explosion of its progenitor star were asymmetric, resulting in a rapid change of the quadrupole moment of the exploding star, and hence, in an associated burst of GR with typical dominant frequency ~ 1 kHz. An expected dimensionless amplitude of GR from such a source, at a distance of about ~ 15 Mpc, is then $\lesssim 10^{-21}$. But supernova explosions can be highly symmetric and, therefore, be poor emitters of GR. Nonetheless, historically, these were the most important sources of GR considered for detection by the early bar detectors.

A new class of GR emitters was considered by Clark and Eardley [1] in the form of coalescing stars of a binary system. A binary should be a strong emitter of GR if the component stars are compact, say, two neutron stars, a neutron star and a black hole, or two black holes. Since the mass quadrupole of a binary system continually changes as the component stars rotate around their common center of mass, a continuous wave of GR would be emitted by the system. However, as more and more of the gravitational binding energy of its orbit gets liberated to GR, the binary coalesces faster and faster. Thus, both the amplitude and the frequency of the emitted radiation will continually increase as the coalescence advances. The resultant wave form, now famous as the chirp, is therefore inherently broadband in nature. Since any interferometric detector could be made to operate over a range of frequencies, it would be ideally suited to detect the chirp. It was Thorne [2] who emphasized the importance of such inherently broadband sources for the present-day laser interferometric GR detectors.

For a narrow-band detector, it is possible for a signal of the burst type to stand above the detector noise. But

*Electronic address: kanti@iucaa.ernet.in

†Electronic address: sanjeev@iucaa.ernet.in

even here, for bar detectors, a maximal signal-to-noise ratio is obtained by using optimal filters [2,3]. However, it is certain that a broadband signal of the coalescing binary will be buried deep in the noise of a broadband detector because it is always difficult to suppress any wideband white noise compared to narrow-band white noise. Consequently, a special technique, matched filtering, needs to be used to detect such signals. Since the GR wave form emitted by the binary is known to high accuracy, the cross correlation of the expected wave form with the detector output would peak depending on how “closely” the filter “matches” the signal picked up by the detector. That is to say, when the detector output and a “prepared filter” (expected wave form) are cross correlated, those values of the parameters (used in preparing the filter) which closely correspond to the “actual” or the signal values would maximize the cross correlation.

The energy and the angular momentum losses of the binary to GR have long been calculated by Peters and Mathews [4] and Peters [5] in the Newtonian approximation. Based on this, a Newtonian approximation to the wave form was obtained by Clark and Eardley [1] and has, since then, been the backbone of the GR detection program, which has in the recent past gained momentum with numerous encouraging results from various feasibility studies of the prototypes of future laser interferometric detectors. In Sec. II, we describe the salient features of the matched-filtering technique for the Newtonian wave form. This section also lists various useful formulas in terms of astronomical units of solar mass and 10^7 cm s as units of mass and orbital radius, respectively. These formulas have not appeared in print in this form earlier, and it is hoped that formulas in this section will serve as ready references for further work. Here, we note that the Newtonian wave form is completely specified by a single parameter, called the mass parameter (see Sec. II). The frequency and the amplitude of the chirp to $v/c \approx m/a$ order, where v is the typical velocity in a binary of total mass m whose component stars are separated by orbital distance a , then depend only on the mass parameter. Consequently, the coalescence time t_C defined as the time taken by the binary with an initial radius a_0 to completely coalesce, can be determined from the mass parameter alone (see Sec. II). Needless to say, this feature of the Newtonian approximation of the chirp has played an important role in the development of signal-detection algorithms for the matched-filtering technique (see Schutz and references therein [6]).

However, the existence of a mass parameter implies that, using the Newtonian approximation and the matched-filtering technique, it is not possible to extract from the signal any information about the masses of the components of the binary. However, the post-Newtonian (PN) terms contain this information and should be incorporated in the matched-filtering analysis to get this vital piece of information. However, terms containing higher powers of v/c , the post-Newtonian terms, become appreciable only during the final stage of coalescence of the binary, at which stage of the evolution of the binary the orbital frequency would be $\gtrsim 500$ Hz. With higher-order terms becoming appreciable, the equation of motion,

energy- and angular-momentum-conservation laws, and the Kepler law for the orbital frequency all get modified. Consequently, the Newtonian approximation to the chirp would appreciably differ from the actual wave form, and this would affect the signal-to-noise ratios of the detection using the matched-filtering method if a Newtonian filter were used. This, however, happens only for the high-frequency part of the signal, and the binary spends very little time in this range of frequencies. So the actual signal, which contains these PN terms, would differ from the Newtonian filter at sufficiently high frequencies. Since, a PN filter is a better approximation to the actual wave form detected by the detector, it is essential to compute the chirp to the required level of accuracy. Following Epstein and Wagoner [7], Wagoner and Will [8] (WW) computed the PN chirp of the GR emitted by binary. Also, Krolak [9] calculated amplitudes averaged over orientations of the source and the detector and gave signal-to-noise ratios for the detector operated with the standard recycling mode. He has also shown that at coalescence the eccentricity of the orbit and the tidal effects can be neglected.

Notation and units

We adopt the following conventions.

The distance R between the observer and the radiation-emitting binary is measured in units of 100 Mpc = 3.0856×10^{26} cm. The angle between the normal to the orbital plane of the binary and the line of sight to the observer is denoted by i . We also assume that the orbit of the binary is a circularized one and that the tidal effects are unimportant. The orbital angular frequency is denoted by ω and the orbital frequency is denoted by f_{orb} , $\omega = 2\pi f_{\text{orb}}$. The period of the binary is denoted by P . The orbital radius a of the binary is measured in units of 10^7 cm. All masses are measured in units of solar mass, $M_{\odot} \equiv 2 \times 10^{33}$ g [for example, total mass m of the binary, reduced mass μ , mass parameter \mathcal{M} (see below), etc.] We limit ourselves to considering stars of mass $0.5 - 10.0 M_{\odot}$. The dimensionless strength of GR, which is considered here as a metric perturbation, is measured in units of 10^{-23} .

II. NEWTONIAN ANALYSIS

We consider two point masses m_1 and m_2 going around each other in a circular orbit under their mutual gravitational influence. In Newtonian theory, the masses are confined to a plane in an elliptical orbit. Therefore, if the plane of the orbit and the orientation of the ellipse in the plane are specified, only the parameters which describe the ellipse remain to be given. We assume that radius of the circular orbit is a and the eccentricity is zero. In Newtonian theory they would be constants of motion.

In the general theory of relativity, however, the system will emit gravitational waves and lose energy. The back reaction will then make a change slowly with time. The gravitational binding energy of this system is

$$E = - \frac{Gm_1 m_2}{2a} . \quad (2.1)$$

As the system loses energy, that is, as E becomes more negative, the distance between two stars must decrease. In the system of units defined at the end of Sec. I, the rate of decay of the orbital radius is given by the equation

$$\frac{da}{dt} = -0.125 \left[\frac{\mu m^2}{a^3} \right], \quad (2.2)$$

where

$$m = m_1 + m_2 \quad (2.3)$$

is the total mass of the stars and

$$\mu = \frac{m_1 m_2}{m} \quad (2.4)$$

is the reduced mass. The instantaneous frequency of GR is easily obtained from Kepler's law:

$$P = 1.719 \left[\frac{a^3}{m} \right]^{1/2} \times 10^{-2} \text{ s}, \quad (2.5)$$

where P is the instantaneous period of the orbit. Therefore

$$f(a) \equiv 2f_{\text{orb}} \quad (2.6a)$$

$$= 1.1635 \left[\frac{m}{a^3(t)} \right]^{1/2} 100 \text{ Hz}. \quad (2.6b)$$

Henceforth, we shall take the lower cutoff frequency of a GR detector to be 100 Hz, which is the conservative assumption made by some groups. However, the projects of the Italo-French group VIRGO and the Laser Interferometric Gravity Wave Observatory (LIGO) expect to go down to even as low as 10 Hz; then our calculation will provide lower bounds on the signal-to-noise ratio.

To deduce the wave form we need to obtain the orbital radius a as a function of time. This needs, then, to be substituted in the expression for h_+ or h_\times . This procedure, however, need not be followed as Eq. (2.2) is exactly integrable and

$$a(t) = a_0 \left[1 - \frac{t}{t_C} \right]^{1/4}, \quad (2.7)$$

where a_0 is the initial radius at $t=0$. However, if we start measuring the time t when the gravitational-wave frequency reaches 100 Hz, i.e., $t=0$ when $f(a_0)=100$ Hz, then

$$t_C = 3\mathcal{M}^{-5/3} \text{ s}, \quad (2.8)$$

where t_C is the coalescence time defined as the time spent by the binary from 100 Hz till the final coalescence. The mass parameter \mathcal{M} is defined by the equation

$$\mathcal{M} = \mu^{3/5} m^{2/5}. \quad (2.9)$$

By substituting this in Eq. (2.6b) we obtain, for the frequency of GR,

$$f(t) = 100 \left[1 - \frac{t}{t_C} \right]^{-3/8} \text{ Hz}, \quad (2.10)$$

and, for the phase integral,

$$2\pi \int_0^t f(t') dt' = 3000 \mathcal{M}^{-5/3} \left[1 - \left(1 - \frac{t}{t_C} \right)^{5/8} \right]. \quad (2.11)$$

The desired wave form in the Newtonian approximation for the plus polarization is

$$h_+^N(t) = 2.86 \left[\frac{m\mu}{Ra(t)} \right] \left[\frac{1 + \cos^2 i}{2} \right] \times \cos \left[2\pi \int_0^t 2f(t') dt' \right], \quad (2.12)$$

and for the cross polarization,

$$h_\times^N(t) = 2.86 \left[\frac{m\mu}{Ra(t)} \right] \cos i \sin \left[2\pi \int_0^t 2f(t') dt' \right]. \quad (2.13)$$

It is observed that in the Newtonian case both the amplitude and phase of the wave form depend only on the particular combination of the masses given by the mass parameter \mathcal{M} , and not on the individual masses.

III. POST-NEWTONIAN ANALYSIS

The effect of the PN term on the wave form manifests itself in two ways: (a) the decay of the orbit of the system follows the modified Kepler law, resulting in changing the evolution of the frequency as a function of time; and (b), more directly, there is an explicit addition of extra terms containing the first four harmonics of the orbital frequency. We discuss these effects in this section.

By taking into account the PN radiation-reaction effect on the orbit of the binary, WW [7] show that the rate of decay of the orbital radius is given by (in the system of units defined in Sec. I)

$$\frac{da}{dt} \equiv -0.125 \left[\frac{\mu m^2}{a^3} \right] \times \left[1 - 0.007425 \left[\frac{m}{a} \right] \left[\frac{13}{168} - \frac{5\mu}{m} \right] \right]. \quad (3.1)$$

For sufficiently large orbital radii, we recover the Newtonian equation (2.2). On the other hand, the frequency of the emitted radiation is related to the orbital radius a through Eq. (2.6b). Thus,

$$f(a) \equiv f(a_0) \left[\frac{a_0}{a} \right]^{3/2} \left[\frac{1 + \kappa/a_0}{1 + \kappa/a} \right], \quad (3.2)$$

where $\kappa \equiv 0.007425(3m - \mu)$ and a_0 is the initial orbital radius. Therefore, Eqs. (3.1) and (3.2) together determine the instantaneous frequency as a function of time. If we assume a lower cutoff of the laser interferometer of 100 Hz, then in our system of units $f(a_0)=100$ Hz, which specifies for us the a at which to begin the integration of Eq. (3.1). The above equations describe the evolution of the frequency as a function of a . However, we will find it useful to obtain f as a function of time in order that we

may use Brigham's fast Fourier transform (FFT) algorithm which requires sampling of the signal at equal time intervals. To this end we integrate Eq. (3.1) to obtain

$$12At = F(a_0) - F(a), \quad (3.3)$$

where

$$F(a) \equiv 3a^4 + 4Ba^3 + 6B^2a^2 + 12B^3a + 12B^4 \ln(a - B), \quad (3.3a)$$

$$A = 0.125\mu m^2, \quad (3.3b)$$

$$B = 0.007425 \left(\frac{13}{168}m - 5\mu \right). \quad (3.3c)$$

We solve Eq. (3.3) numerically using the bisection method to obtain a as a function of t . The subroutine used is RTBIS of Numerical Recipes [10]. To start the routine the initial guess for a is taken to be the Newtonian value, which can be obtained easily via an analytic ex-

pression. We can now obtain f for any value of t , and in particular we can sample at equal intervals in time. The numerical accuracy is set to be 10^{-9} so that the wave form is adequately sampled towards the final stages of coalescence. The usage of the FFT algorithms becomes almost imperative for colored noise where the signal-to-noise ratios are calculated in the frequency domain.

Following WW, Krolak [9] has given a concise form for the signal from a binary up to second PN order (we follow Will's convention for PN orders [11]; in Krolak's convention the wave form given below is up to first PN order). Writing Krolak's form termwise and replacing his ωt with the more appropriate $\phi(t) = 2\pi \int_0^t f(t') dt'$, we have

$$h_+(t) \equiv \frac{m}{a} h_{1N}^+ + \left(\frac{m}{a} \right)^{3/2} h_{3/2PN}^+ + \left(\frac{m}{a} \right)^2 h_{2PN}^+, \quad (3.4)$$

where

$$h_{1N}^+ = -1.428 \frac{\mu}{R} (1 + \cos^2 i) \cos 2\phi, \quad (3.4a)$$

$$h_{3/2PN}^+ = -0.348 \frac{\mu}{R} \frac{\delta m}{m} \left[\frac{\sin i}{16} (5 + \cos^2 i) \sin \phi + \frac{9}{16} \sin i (1 + \cos^2 i) \sin 3\phi \right], \quad (3.4b)$$

$$h_{2PN}^+ = 0.042 \frac{\mu}{R} \left\{ \left[\left(1 - \frac{3\mu}{m} \right) \frac{\sin^2 i}{3} (3 + \cos^2 i) + \frac{1}{2} \left(\frac{19}{6} - \frac{\mu}{2m} \right) (1 + \cos^2 i) \right] \cos 2\phi \right. \\ \left. + \left[1 - \frac{3\mu}{m} \right] \left(\frac{2}{3} \sin^2 i \right) (1 + \cos^2 i) \cos 4\phi \right\}. \quad (3.4c)$$

For other polarizations we obtain

$$h_\times(t) \equiv \frac{m}{a} h_{1N}^\times + \left(\frac{m}{a} \right)^{3/2} h_{3/2PN}^\times + \left(\frac{m}{a} \right)^2 h_{2PN}^\times, \quad (3.5)$$

where

$$h_{1N}^\times = 2.858 \frac{\mu}{R} \cos i \sin 2\phi, \quad (3.5a)$$

$$h_{3/2PN}^\times = -0.131 \frac{\mu}{R} \frac{\delta m}{m} \cos i \sin i (\cos \phi + 3 \cos 3\phi), \quad (3.5b)$$

$$h_{2PN}^\times = -0.042 \frac{\mu}{R} \left\{ \left[\left(1 - \frac{3\mu}{m} \right) \right] \left[\frac{2}{3} \sin^2 i \right] + \left[\frac{19}{6} - \frac{\mu}{2m} \right] \right\} \cos i \sin 2\phi + \left[1 - \frac{3\mu}{m} \right] \left[\frac{4}{3} \sin^2 i \cos i \right] \sin 4\phi. \quad (3.5c)$$

The first term h_{1N} of either polarization is called the Newtonian part of the PN chirp because most of the contributions to the PN chirp initially come from this term, but at higher frequencies the rest of the terms contribute significantly.

The phase integral $2\pi \int_0^t f(t') dt'$ is evaluated using the subroutine QROMB of Numerical Recipes [10]. The numerical accuracies were checked by comparing results with the analytical Newtonian expressions. In the PN amplitudes there are four components corresponding to one, two, three, and four times the orbital frequency f_{orb} ,

which is given by the Kepler's law

$$f_{\text{orb}} = \frac{1}{2\pi} \left(\frac{m}{a^3} \right)^{1/2} \left(1 + \frac{3m - \mu}{2a} \right)^{-1}, \quad (3.6)$$

which has been modified to incorporate PN effects on the binary orbit. It is important to note that these different frequency components begin appearing in the detector output at different times. The first term that will be sensed by the detector at 100 Hz will be 4ϕ , then 3ϕ , 2ϕ , and ϕ . This means that one must start considering the

signal when $4f_{\text{orb}} = 100$ Hz. However, one finds that this is not necessary and we can begin considering the signal later when the orbital frequency reaches the value $\frac{1}{3} \times 100$ Hz, since the integrated contribution of the 4ϕ term to the signal-to-noise ratio is 1 part in 10^5 during the period $\frac{1}{4} \leq f_{\text{orb}}/100 \text{ Hz} \leq \frac{1}{3}$. Therefore, we begin the calculations when $f_{\text{orb}}/100 \text{ Hz} = \frac{1}{3}$. As the frequency increases at later times, the 2ϕ and ϕ terms are switched on at appropriate epochs. At the upper end, which is taken to be 2000 Hz, the first term to go out of the detector range is the 4ϕ term, followed by 3ϕ , 2ϕ , and finally ϕ . However, here we stop the calculations when $f_{\text{orb}} = 1000$ Hz, so that the contribution of the ϕ term is not considered beyond this limit. We argue that other effects such as tidal forces will dominate at this stage, and the simple model of the two point masses may not serve well. The numerical analysis switches on and off various terms accordingly.

IV. THE SIGNAL-TO-NOISE RATIOS FOR THE POST-NEWTONIAN WAVE FORM

A. Comparison with the Newtonian S/N ratios

As mentioned earlier, the matched-filtering technique happens to be the appropriate technique when the wave form is known. This technique involves correlating the data with a known copy of the expected wave form called the filter. In linear filtering, matched-filtering maximizes the signal-to-noise ratio, which is the maximum of the correlation. The matched filter is proportional to the predicted wave form if the noise spectrum is white, otherwise it is different. If $\tilde{h}(f)$ is the Fourier transform of the expected wave form $h(t)$, which has support over the time interval $[0, T]$, and $S_h(f)$ is the one-sided spectral density of noise, then the Fourier transform $\tilde{q}(f)$ of the filter is given by

$$\tilde{q}(f) = \frac{\tilde{h}(f)}{S_h(f)}. \quad (4.1)$$

The signal-to-noise ratio is then

$$\left[\frac{\mathcal{S}}{\mathcal{N}} \right]^2 = 2 \int_0^\infty \frac{|\tilde{h}(f)|^2}{S_h(f)} df \quad (4.2)$$

The S/N ratio can be regarded as a norm on the space of wave forms.

In this section we compute the signal-to-noise ratios when a PN signal is filtered out by the matched filter. We will assume two forms for the spectral density of the noise: (a) white, constant spectrum S_0 ; (b) noise present when the detector is operated in the standard recycling mode. Krolak has already addressed this problem by computing the S/N ratios averaged over all possible orientations of the source and detector and over the period of the orbit of the binary. Our calculation, on the other hand, extends to the evaluation of S/N ratios for a range of masses of the stars, orientations of the orbital plane of the binary, and orientations of the detector.

As we remarked earlier, the amplitude of the Newtonian

chirp wave form depends only on the mass parameter and not on the component masses of the binary. Thus, for the same mass parameter, different values of m_1 and m_2 are permitted by the Newtonian approximation. On the other hand, the post-Newtonian approximation does depend on m_1 and m_2 explicitly through the terms of the order $(m/a)^{3/2}$ and $(m/a)^2$. Since the sign of the PN- 2ϕ term is opposite to that of the Newtonian term, it has the effect of reducing the signal-to-noise ratios considerably in the PN case, in spite of the fact that the PN term has $(m/a)^2$ dependence. The second reason for the decrease of the signal-to-noise ratio for the PN case is that the coalescence time is less in this approximation. So neglecting the PN term leads to an overestimation of the signal-to-noise ratio.

Various factors affecting the value of the norm of the chirp wave form can be estimated as follows. First, we note that the mass difference δm affects the value of the overall amplitude in two ways—by adding a term proportional to δm and by, for a large mass difference, implying a shorter coalescence time and, hence, a smaller initial orbital radius (corresponding to a 100-Hz frequency). Although the contribution of this term is suppressed by the factor 0.384, a smaller orbital radius increases the contribution of this term considerably. At smaller orbital radii, however, the term proportional to $(m/a)^2$ contributes more. Basically, it is the coalescence time that is reduced as a result of the large mass difference, and hence, the signal-to-noise ratio with a PN correction can be considerably less than the corresponding Newtonian value.

This prompts the following comparison of the two norms—one Newtonian and the other post-Newtonian.

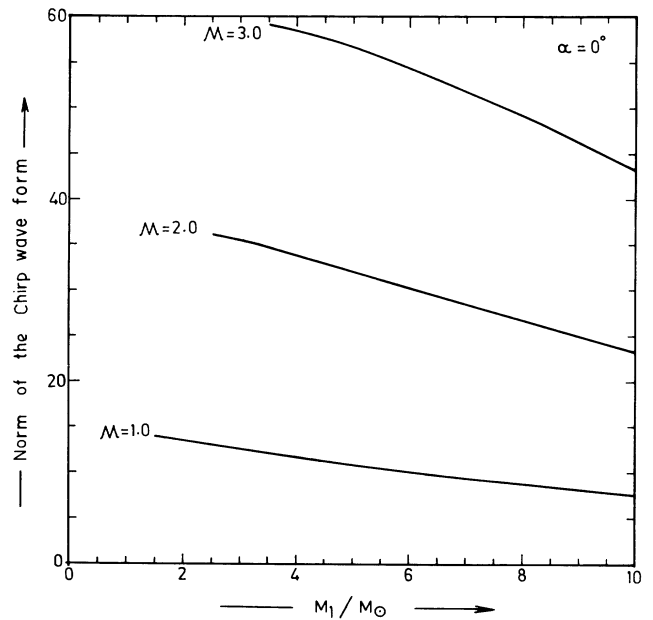


FIG. 1. Norm of the post-Newtonian chirp wave form plotted for fixed values of the mass parameter \mathcal{M} as a function of mass m_1 . $\mathcal{M} = 1.0, 2.0,$ and $3.0M_\odot$. The corresponding norms for the Newtonian case are 19.6, 62.20, 122.23, respectively. The angle of orbital inclination is $i = 0^\circ$.

To get an idea of the numbers involved, we consider the case for white noise with $S_h(f) = S_0 = 10^{-46} \text{ Hz}^{-1}$ and fix the distance of the binary at 100 Mpc. We vary the individual masses of the stars in such a way that the mass parameter is kept constant. This implies that the Newtonian wave form remains fixed, while the PN norm will vary. The behavior of post-Newtonian norms for fixed mass parameters is shown in Fig. 1. The figure shows three curves for mass parameter values $\mathcal{M} = 1.0, 2.0,$ and 3.0 for the orbital inclination angle $i = 0^\circ$. Since the norm is a symmetric function of the masses m_1 and m_2 , the curves are drawn for $m_2 \geq m_1$ only. It is seen that the norm for the PN wave form, on the whole, is less than the corresponding Newtonian value and decreases as the mass difference increases. This behavior may be attributed to the reduction in the coalescence time. The corresponding Newtonian values of the norm for three different values of the mass parameter are 19.6, 62.20, and 122.23, respectively.

B. The basic formalism of S/N ratios

It is useful and instructive to single out the case in which we consider only the 2ϕ term of the full wave form. The ratios then can be stated semianalytically, and this case is applicable to a wide range of parameters. In this section we first give a brief review of the spectral density of the noise when the detector is operating in the standard recycling mode and then derive the formulas which express S/N ratios as a function of detector orientation.

1. Spectral density of the noise for standard recycling

Drever [12] has devised a method for improving the sensitivity of either a Michelson delay line or a Fabry-Perot arrangement when the mirror reflectivities permit storing light for much longer than a half-period. The basic idea is to extract the light after a half-period, when further storage is self-defeating, and reinsert it back. The method is known as standard recycling. The spectral density of the noise for this mode of operation can be expressed by the formula

$$S_h(f) = \begin{cases} S_0 \left[1 + \left(\frac{f}{f_k} \right)^2 \right], & f \geq f_s, \\ \infty, & f < f_s, \end{cases} \quad (4.3a)$$

$$(4.3b)$$

where f_s is called the ‘‘seismic cutoff.’’ The noise below f_s rises rapidly with decreasing f and can be virtually taken to be infinite.

We again assume that the lower cutoff frequency f_s is 100 Hz. The quantity f_k is known as the ‘‘knee frequency.’’ We choose its value to be $1.44f_s$, which maximizes the S/N ratio for coalescing binaries for the Newtonian wave form. For a detector with an arm length of 3 km, effective laser power of 100 W, end mirror reflectivity of $\sim 5 \times 10^{-5}$, and operating at the green-light frequency (reduced wavelength $\lambda \sim 0.0818 \mu\text{m}$), the value of S_0

turns out to be $6.5 \times 10^{-48} \text{ Hz}^{-1}$ (see Thorne [2] for a detailed discussion).

2. S/N ratio as a function of detector orientation

We consider here two cases: (i) the spectral density of noise is a constant (white noise), and (ii) the spectral density is that of standard recycling. To this end, we adopt the following definition for a scalar product. Let $\mathcal{F}(t)$ and $\mathcal{G}(t)$ be square-integrable functions over the time axis and $\tilde{\mathcal{F}}(f)$ and $\tilde{\mathcal{G}}(f)$ the corresponding Fourier transforms. We define the scalar product between \mathcal{F} and \mathcal{G} to be

$$\langle \mathcal{F}, \mathcal{G} \rangle = 2 \int_0^\infty \frac{\tilde{\mathcal{F}}(f) \tilde{\mathcal{G}}^*(f)}{S_h(f)} df, \quad (4.4)$$

where the * denotes complex conjugation. For white noise, the scalar product reduces to

$$\langle \mathcal{F}, \mathcal{G} \rangle = S_0^{-1} 2 \int_0^\infty \mathcal{F}(t) \mathcal{G}(t) dt \quad (4.5)$$

in the time domain. For a matched filter $\mathcal{F} = \mathcal{G}$ and we may write

$$\langle \mathcal{F}, \mathcal{F} \rangle = \|\mathcal{F}\|^2, \quad (4.6)$$

where $\|\mathcal{F}\|$ is called the norm of \mathcal{F} . The response of the detector is

$$R = \frac{\delta l}{l}, \quad (4.7)$$

where δl is the change in arm length of the interferometer. R is in general a linear combination of the two polarization amplitudes $h_+(t)$ and $h_\times(t)$ and a function of angles describing the orientations of the detector. More specifically, following Schutz and Tinto [13] we introduce two sets of orthogonal Cartesian coordinate systems: (i) detector axes (x, y, z) , with the axis of the detector lying in the (x, y) plane and the x axis bisecting the two arms; (ii) wave axes (X, Y, Z) , with the Z axis aligned to the direction of propagation of the wave and the (X, Y) plane containing the polarization ellipse. The Euler angles (θ, ϕ, ψ) give the orientation of the wave axes with respect to the detector axes. The response of the detector $R(t)$ is given by

$$R(t) = F_+(\theta, \phi, \psi) h_+(t) + F_\times(\theta, \phi, \psi) h_\times(t), \quad (4.8)$$

where

$$F_+(\theta, \phi, \psi) = \cos 2\phi \cos \theta \sin 2\psi + \frac{1}{2} \sin 2\phi (1 + \cos^2 \theta) \cos 2\psi, \quad (4.9a)$$

$$F_\times(\theta, \phi, \psi) = \cos 2\phi \cos \theta \cos 2\psi - \frac{1}{2} \sin 2\phi (1 + \cos^2 \theta) \sin 2\psi. \quad (4.9b)$$

Now, assuming that we use a matched filter, the S/N ratio is given in our notation by

$$\left(\frac{S}{N} \right)^2 = \langle R, R \rangle = \|R\|^2, \quad (4.10)$$

whatever the noise spectrum. The signal-to-noise ratio is now

$$\begin{aligned} \left[\frac{S}{N} \right]^2 &= \|R\|^2 \\ &= F_+^2 \|h_+\|^2 + F_\times^2 \|h_\times\|^2 + 2F_+ F_\times \langle h_+, h_\times \rangle. \end{aligned} \quad (4.11)$$

Numerical calculations show that the cross term $\langle h_+, h_\times \rangle$ is negligible compared to $\|h_+\|^2$ or $\|h_\times\|^2$. We do the integration in the frequency domain with the upper cutoff at 2000 Hz. We find that the term $\langle h_+, h_\times \rangle \sim 10^{-5} - 10^{-7}$, while $\|h_+\|^2$ and $\|h_\times\|^2$ are $\sim 10^2$ or 10^3 . Typically, if we take each of the individual masses of the stars to be $1M_\odot$, then $\langle h_+, h_\times \rangle \sim 10^{-6}$ for white noise and 4.3×10^{-7} for noise pertaining to standard recycling. Even for higher values of masses the result generally remains true. We have checked this result numerically up to $10M_\odot$. The underlying reason for this is that the set of functions $\sin(n\phi)$ and $\cos(n\phi)$, n a positive integer, form an orthogonal set over $[0, 2\pi]$, or in general over $[0, 2m\pi]$ where m is a positive integer, under the L_2 scalar product. Although the functions appearing in $h_+(t)$ or $h_\times(t)$ are not strictly sinusoidal, since f is not constant in time, they are more or less so over a single oscillation, except possibly at higher frequencies where, anyway, the integration time is small. Similarly, $S_h(f)$, which mathematically plays the role of the weight function and which is not constant for the recycling mode, does not appreciably affect the result. Therefore, to a good approximation we can express the full S/N ratio in terms of S/N ratios corresponding to individual polarizations. Thus,

$$\left[\frac{S}{N} \right]^2 = F_+^2 \left[\frac{S}{N} \right]_+^2 + F_\times^2 \left[\frac{S}{N} \right]_\times^2, \quad (4.12)$$

where

$$\left[\frac{S}{N} \right]_+^2 = \|h_+\|^2 \quad \text{and} \quad \left[\frac{S}{N} \right]_\times^2 = \|h_\times\|^2. \quad (4.13)$$

3. The computation of S/N ratios

a. S/N ratios for the h_{1N}^+ and h_{1N}^\times terms. We treat the case for these terms separately for the following two reasons: (a) they make a dominant contribution to the full S/N ratio; (b) the S/N ratio can be obtained in a semianalytic manner, i.e., the angles of orientation of the binary orbit and the detector appear analytically in the formula while the rest of the parameters are treated numerically. The semianalytic nature of the formula helps in widening its applicability to a continuous range of the parameters that appear analytically in the formula.

Since each of the polarization amplitudes is restricted to a single term, the following simplification occurs:

$$\left[\frac{S}{N} \right]^2 = F_+^2 \left[\frac{1 + \cos^2 i}{2} \right]^2 A_+^2 + F_\times^2 \cos^2(i) A_\times^2, \quad (4.14a)$$

where

$$A_+^2 = \|A \cos 2\phi\|^2, \quad (4.14b)$$

$$A_\times^2 = \|A \sin 2\phi\|^2, \quad (4.14c)$$

$$A = 2.858 \left[\frac{\mu}{R} \right]. \quad (4.14d)$$

However, it is easy to see that $A_+^2 = A_\times^2$ and that each is equal to $(S/N)_+^2 = (S/N)_\times^2$ when the orbital plane of

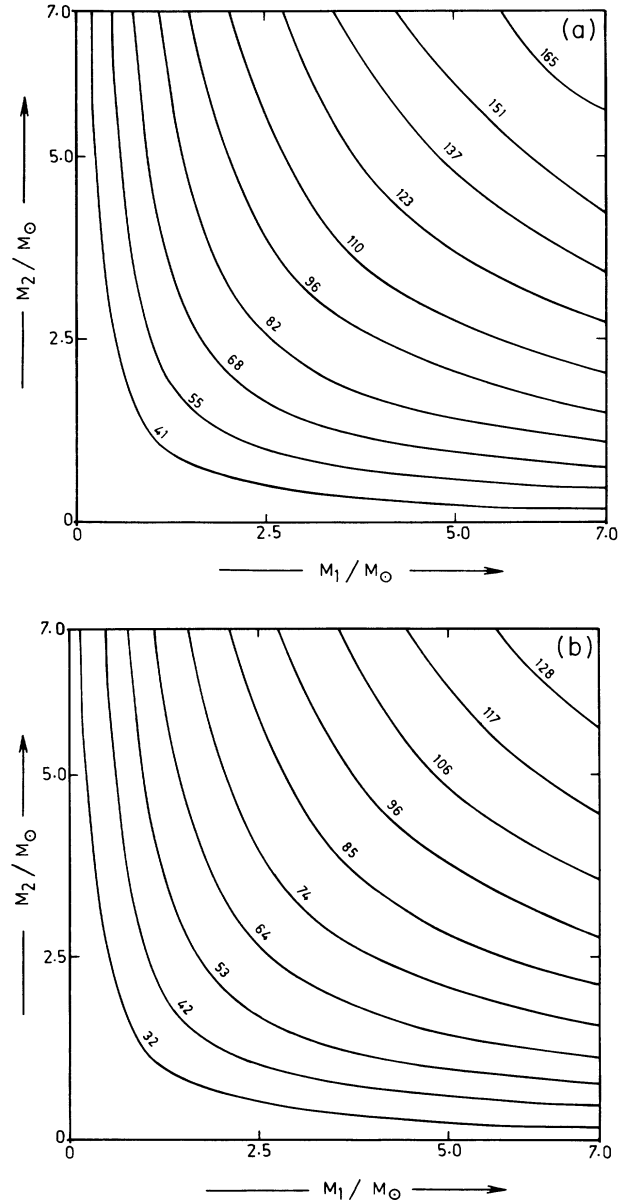


FIG. 2. Contour plots show the signal-to-noise ratio $(S/N)_{i=0}$ for the post-Newtonian chirp wave form as a function of m_1 and m_2 . (a) corresponds to white noise, while (b) corresponds to colored noise of standard recycling with $f_k = 144$ Hz. The white-noise level is taken constant at $S_0 = 9.6 \times 10^{-49} \text{ Hz}^{-1}$, which is also the level of the colored noise at 100 Hz. The (S/N) ratio for arbitrary orientations of detector and source can be calculated from $(S/N)_{i=0}$ from Eq. (4.15).

the binary coincides with the plane of the sky, i.e., when $i=0^\circ$. If we denote this common quantity by $(S/N)_{i=0}^2$ then, taking the square root of Eq. (4.14a), we get

$$\frac{S}{N} = \left[F_+^2 \left[\frac{1 + \cos^2 i}{2} \right]^2 + F_\times^2 \cos^2 i \right]^{1/2} \left[\frac{S}{N} \right]_{i=0}. \quad (4.15)$$

We now need to specify $(S/N)_{i=0}$ so that the S/N ratios can be computed from Eq. (4.15). In Figs. 2(a) and 2(b) we give contour plots of $(S/N)_{i=0}$ as a function of m_1 and m_2 for the detector orientation $\theta=\phi=0$. In Fig. 2(a) the contour plot corresponds to a white-noise level fixed at $S_0=9.6 \times 10^{-49} \text{ Hz}^{-1}$. We have chosen the value of

S_0 to be the same as that of colored noise at 100 Hz and obtained it by setting $f=100 \text{ Hz}$ in Eq. (4.3a). In Fig. 2(b) the contour plot pertains to colored noise for the standard recycling case. From the contour plots it can be seen that the S/N ratio for the white noise is in general higher than in the standard recycling case. This is due to the arbitrary normalization of assuming the white-noise level S_0 to be the minimum of the noise level in the standard recycling case. For standard recycling, the higher frequencies, $f \gtrsim f_k$ in the wave form, are suppressed in their contribution to the S/N ratio.

b. The S/N ratios for the full wave form. The analysis for the full wave form on lines of the previous

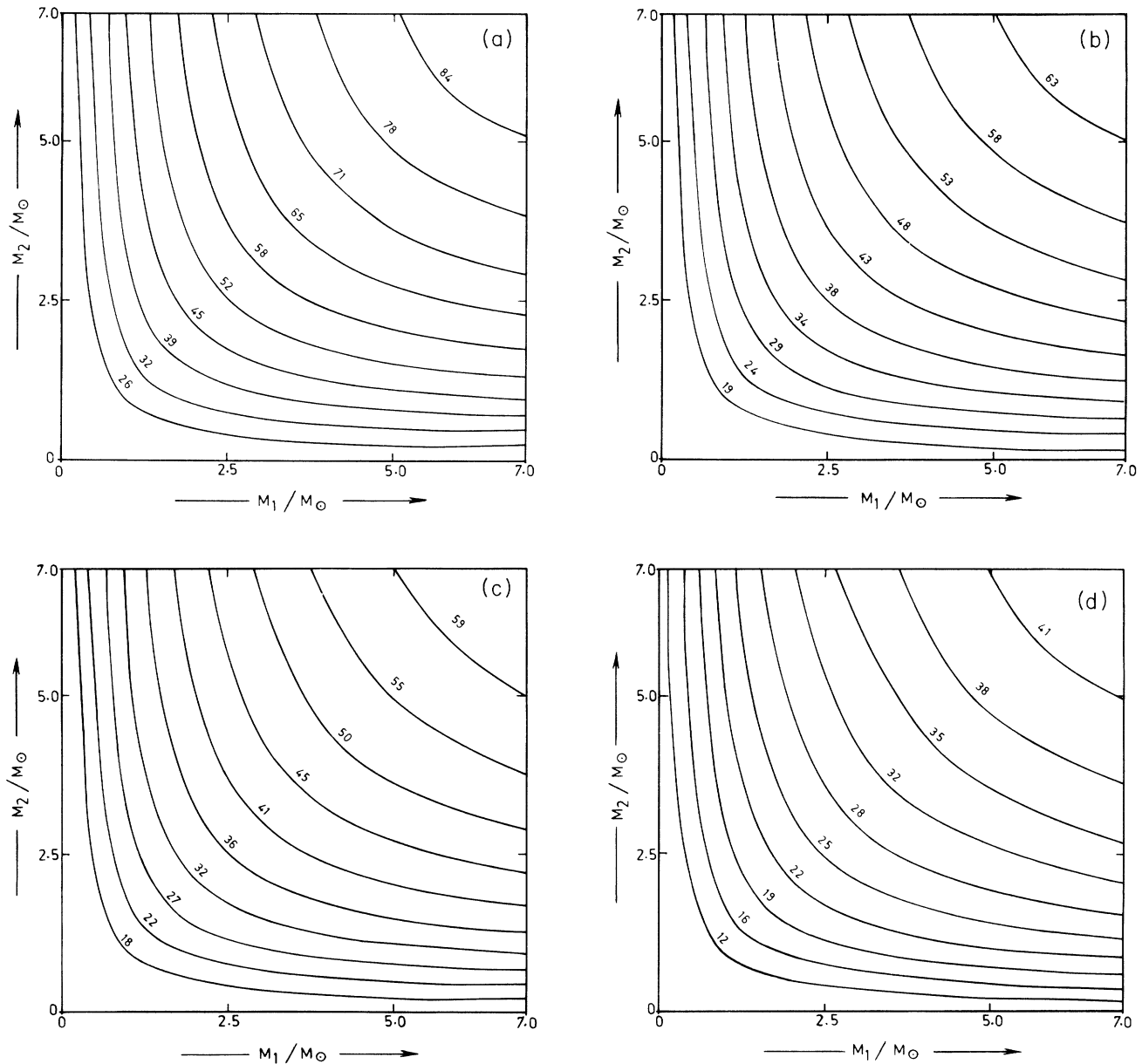


FIG. 3. Contour plots for S/N for the full post-Newtonian wave form for the standard recycling case with $f_k = 144 \text{ Hz}$. The contour plots are given for various polarizations and orbital angles of inclination of the source: (a) + polarization and $i=0^\circ$; (b) + polarization and $i=45^\circ$; (c) \times polarization and $i=45^\circ$; (d) + polarization and $i=90^\circ$.

case is not very convenient because the full wave form has a complicated dependence on the orbital inclination angle i . We consider here three values of i : (a) $i=0^\circ$, (b) $i=45^\circ$, (c) $i=90^\circ$. In case (a), since the orbital plane of the binary coincides with that of the sky, the wave is circularly polarized and the amplitudes of the two polarizations are equal. This results in

$$\left(\frac{S}{N}\right)_+ = \left(\frac{S}{N}\right)_\times, \quad (4.16)$$

and only one of the quantities needs to be specified to determine the full S/N ratio. Case (b) is a general case where $(S/N)_+$ and $(S/N)_\times$ are unequal, and thus both have to be specified in order to get the full S/N ratio. In case (c) we find that $(S/N)_\times=0$. This is due to the particular choice of the coordinate system, and only $(S/N)_+$ determines the full S/N ratio. For the general case of $0^\circ < i < 90^\circ$ both $(S/N)_+$ and $(S/N)_\times$ are needed to determine the S/N ratio. In Figs. 3(a)–3(d) we display the contour plots for the relevant S/N ratio, as described above, for standard recycling and for the detector orientation given by $\theta=\phi=0^\circ$. The general trend is for the S/N ratio to decrease as i increases from 0° to 90° , i.e., as the orbital plane inclines more and more to the plane of the sky. Although this is not shown here we have checked that similar results hold when the noise is white. The basic reason for this behavior is that when $i=0^\circ$ both polarizations contribute maximally to the S/N ratio. As the plane of the orbit turns away both polarization amplitudes decrease, reducing the S/N ratio. For $i=90^\circ$, the contribution of the cross polarization is zero and one gets a low value for S/N .

The question is how these full results compare with the h_{1N}^+ and h_{1N}^\times results obtained in (i) from Eq. (4.15). We find that Eq. (4.15) gives better results when the masses of the stars are low. For example, if the masses are $\lesssim 2M_\odot$ each, then Eq. (4.15) overestimates by about 10% the S/N ratio obtained for the full wave form. This is mainly due to the linear contribution in the amplitude of the h_{1N}^+ and h_{1N}^\times terms when one includes the 2ϕ terms from h_{2PN}^+ and h_{2PN}^\times . Although other ϕ , 3ϕ , and 4ϕ terms contribute positively to total the S/N ratio, this contribution is quadratic and hence small compared to the linear addition. For each of the individual masses $\simeq 5M_\odot$, Eq. (4.15) overestimates the S/N ratio by as much as 20%.

V. CONCLUDING REMARKS

We observe that the full post-Newtonian S/N ratio reduces from its Newtonian counterpart by about 15% for stars with masses of $\sim 1M_\odot$. This is valid only when we consider a wide range of frequencies for detection, from 100 to 2000 Hz. If we, however, reduce the upper limit from 2000 to 400 Hz, the S/N ratios for the Newtonian and the post-Newtonian cases differ very little. In the PN case there is very little contribution to the S/N ratio over 400 Hz. The reduction in the S/N ratio here is mainly due to the reduction in the integration time. This has the following implication: for a broadband width from 100 to 2000 Hz, the reduction in the S/N ratio will lead to a reduction in the distance to which we can detect a binary, and hence to a reduction in the event rate as predicted from the Newtonian analysis.

Comparing our analysis with Krolak's, we find that we arrive at similar numbers. However, in our analysis detailed computations have been carried out in the PN approximation to get the decay of the orbit. Further, the S/N ratios are computed for various values of the masses m_1 and m_2 , the orbital plane inclination i , and various detector orientations θ and ϕ .

All this analysis is a precursor to the more detailed analysis to follow, where one can gauge how efficiently a "bank of Newtonian filters" [14] can filter out a PN signal. This will involve computing scalar products defined in this paper: the scalar product between a PN signal and a Newtonian filter. However, the analysis is expected to be more complex since the signal now involves the individual masses of the stars. It is possible that the maximum of the cross correlation may occur when the mass parameters of the signal and filter are mismatched. A similar situation was encountered when the mass parameters of the filter and signal did not match [14]. Then the cross correlation peaked only when there was a time shift and phase shift between the signal and the filter. This effect was due to the nonzero covariance between the parameters of the signal.

ACKNOWLEDGMENTS

We thank C-DAC, Pune, India, for partly supporting this work.

[1] J. P. A. Clark and D. M. Eardley, *Astrophys. J.* **215**, 311 (1977).
 [2] K. S. Thorne, in *300 Years of Gravitation*, edited by S. W. Hawking and W. Israel (Cambridge University Press, Cambridge, England, 1987).
 [3] J. P. Richard and W. M. Folkner, in *The Detection of Gravitational Waves*, edited by D. G. Blair (Cambridge University Press, Cambridge, England, 1991).
 [4] P. C. Peters and J. Mathews, *Phys. Rev.* **131**, 435 (1963).
 [5] P. C. Peters, *Phys. Rev.* **136**, B1224 (1964).

[6] B. F. Schutz, in *The Detection of Gravitational Waves*, edited by D. G. Blair (Cambridge University Press, Cambridge, England, 1991).
 [7] R. Epstein and R. V. Wagoner, *Astrophys. J.* **197**, 717 (1975).
 [8] R. V. Wagoner and C. M. Will, *Astrophys. J.* **210**, 764 (1976).
 [9] A. Krolak, in *Gravitational Wave Data Analysis*, edited by B. F. Schutz (Kluwer, Dordrecht, 1989).
 [10] W. H. Press, B. P. Flannery, S. A. Teukolsky, and W. T.

Vetterling, *Numerical Recipes: The Art of Scientific Computing* (Cambridge University Press, Cambridge, England, 1986).

[11] C. W. Lincoln and C. M. Will, *Phys. Rev. D* **42**, 1123 (1990).

[12] R. W. P. Drever, in *Gravitational Radiation*, edited by N.

Deruelle and T. Piran (North-Holland, Amsterdam, 1983).

[13] B. F. Schutz and M. Tinto, *Mon. Not. R. Astron. Soc.* **224**, 131 (1987).

[14] B. S. Sathyaprakash and S. V. Dhurandhar, *Phys. Rev. D* **44**, 3819 (1991).